ORGANIC CHEMISTRY FRONTIERS

CCS 中国化学会 CHINESE CHEMICAL SOCIETY

SIOC 1950

ROYAL SOCIETY OF CHEMISTRY

RESEARCH ARTICLE

View Article Online
View Journal | View Issue

Cite this: *Org. Chem. Front.*, 2026, **13**, 550

Scalable manganese-electrocatalytic three-component heteroarene azidoalkylation *via* a polarity-reversing radical cascade

Qi-Liang Yang, *†[a] Zhong-Xu Zhang,†[a] Ye Zhu,[a] Zu-Lin Qiao,[a] Xin Liu,[a] Rong Wang,[a] Shu-Xian Liu,[a] Er-Jun Hao, [a] Peng Xiong*[b] and Hai-Ming Guo *[a]

Received 13th September 2025,
Accepted 11th November 2025

DOI: 10.1039/d5qo01302j

rsc.li/frontiers-organic

An electrochemical approach has been established for azidoalkylation of heteroarenes using unactivated alkenes and NaN_3 *via* a polarity reversal radical cascade strategy, enabling the synthesis of diverse C6-azidoalkylated purine derivatives that possess significant yet unexplored medicinal relevance. This three-component Minisci-type reaction was promoted by the $Mn^{III/II}$ redox couple and involved the *in situ* selective addition of an electrophilic $N_3^{\bullet}$ to an alkene, generating a nucleophilic C-centered radical that rapidly coupled with a variety of heteroarenes to form the corresponding adducts. The present method is characterized by a wide substrate scope (90 examples, up to 92% yield), exceptional functional group tolerance, mild reaction conditions, high chemo- and regio-selectivities, facile derivatization of products, and easy scalability. This strategy is applicable to alkenes with various substitution patterns and electronic properties, enabling the efficient synthesis and late-stage derivatization of pharmacologically active molecules, which holds great value in medicinal chemistry. Mechanistic studies support a radical mechanism involving the generation of both azido and β-azido alkyl radicals.

Structural analysis of the U.S. FDA-approved pharmaceutical database reveals that N-heteroarenes are widely prevalent in drug architectures, with purines, pyrimidines, pyridines, indoles, imidazoles, and quinolines being the most common core structures.[1] As a result, late-stage functionalization of complex frameworks containing N-heteroarenes is of paramount importance in drug research and development.[2] In contrast to traditional electrophilic Friedel–Crafts-type reactions, Minisci-type reactions occur *via* nucleophilic radicals, offering distinct selectivity and reactivity.[3] The classical Minisci reaction involves a two-component reaction that adds nucleophilic radicals to electrophilic N-heterocycles. However, coupling an electrophilic radical with an electron-deficient heteroarene is highly unfavorable due to the electrophilic nature of both species. To address this electronic mismatch, Minisci-type multicomponent reactions employing a polarity-reversal strategy have emerged as a powerful solution.[4] By assembling electrophilic radicals, alkenes, and electrophilic heteroarenes in a radical cascade, these reactions enable the incorporation of structurally diverse, C(sp^3)-rich motifs onto electron-deficient N-heterocycles and facilitate the sequential formation of C(sp^3)–C(sp^2) and C(sp^3)–X (X = C,[4a] P,[4c] S,[4d,e] N[4f]) bonds, thereby constructing complex molecular architectures with high atom- and step-efficiency.

The azido group (N_3) is used ubiquitously in chemical biology,[5] medicinal chemistry,[6] peptide chemistry,[7] and materials science[8] (Scheme 1a). It also serves as a versatile synthetic equivalent for a plethora of useful transformations, including reactions with electrophiles and nucleophiles, "click" reactions,[9] aza-Wittig reaction,[10] Staudinger ligation,[11] Curtius rearrangement,[12] Schmidt rearrangement,[13] and C–H bond amination,[14] among others. Thus, the development of sustainable, efficient, and selective methods for incorporating an azido group into complex organic molecules remains highly desirable.[15]

Owing to its high reactivity, the azide radical readily participates in competing parallel reactions or undergoes decomposition.[16] Harnessing the controlled solution-phase reactivity of transient electron-deficient azide species still presents a challenge in modern organic synthesis.[17] In this regard, synthetic methods for azido radical-mediated alkene azidoheteroarylation, particularly through a three-component approach, are

[a]*State Key Laboratory of Antiviral Drugs, Pingyuan Laboratory, Key Laboratory of Green Chemical Media and Reactions, Ministry of Education, Collaborative Innovation Center of Henan Province for Green Manufacturing of Fine Chemicals, School of Chemistry and Chemical Engineering, Henan Normal University, Xinxiang, Henan 453007, China. E-mail: yangqiliang@htu.edu.cn, ghm@htu.edu.cn*
[b]*The Key Laboratory of Chemical Biology of Fujian Province College of Chemistry and Chemical Engineering Xiamen University, Xiamen, Fujian 361005, China. E-mail: pengxiong@xmu.edu.cn*
†These authors contributed equally to this work.

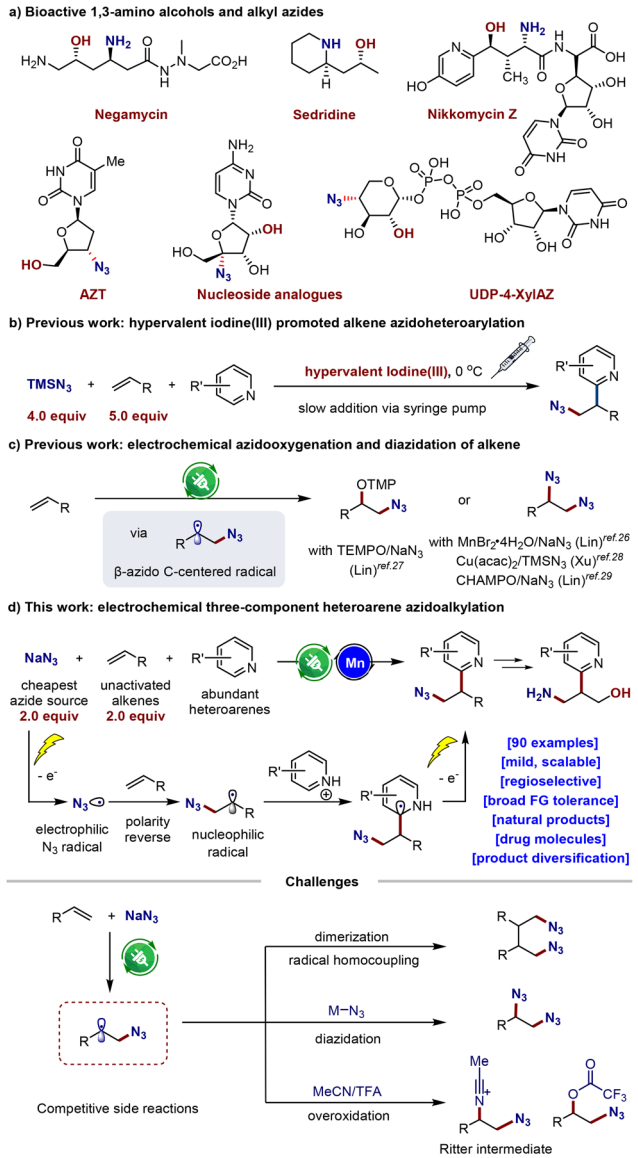

Scheme 1 Background and summary of this study.

scarce and challenging. The groups of Liu[18] and Nagib[19] successively developed an iodine(III) reagent-promoted oxidation system for the azidoheteroarylation of simple aliphatic alkenes, employing $TMSN_3$ and heteroarenes as components (Scheme 1b). Chu's group[20] reported the redox-neutral three-component azidoarylation of styrenes with cyanopyridines and $TMSN_3$ to afford β-azidopyridines *via* organic photoredox catalysis. Despite the above-mentioned progress and other works,[21] these methods suffer from some drawbacks to some extent, such as: (1) the potential explosion risk arising from the combination of chemical oxidants and azide sources, along with the generation of substantial environmentally hazardous waste; (2) the need for specialized techniques, such as the slow addition of $PhI(OAc)_2$ *via* a syringe pump to avoid the rapid formation of $N_3^{\bullet}$ in excessive concentration; (3) the use of a toxic and volatile azidotrimethylsilane reagent; (4) the requirement of a large excess of both the alkene and azide components; and (5) reliance on the use of expensive photocatalysts under blue LED irradiation, facing challenges such as potential health risks,[22] low quantum efficiency, and difficulties in scaling up.[23]

Over the past decade, organic electrosynthesis has emerged as an appealing, energy-efficient, and environmentally sustainable strategy for a wide range of valuable organic transformations, particularly in the difunctionalization of alkenes.[24] The integration of electrochemistry with redox mediators offers a reliable and sustainable approach for generating azide radicals and controlling their reactivity,[25] significantly enhancing the efficacy and selectivity of alkene azido-functionalization. In this context, the Lin group gave a pioneering report on the electrochemical vicinal 1,2-diazidation of alkenes using a $MnBr_2{\cdot}4H_2O/NaN_3$ catalytic system *via* a manganese(II/III) manifold.[26] Subsequently, the same research group also developed an electrochemical azidooxygenation of alkenes using (2,2,6,6-tetramethylpiperidin-1-yl)oxyl (TEMPO) as an aminoxyl catalyst, involving TEMPO-N_3-mediated azidyl transfer.[27] Recently, the Xu group disclosed a copper(II)-catalyzed electrochemical protocol to generate 1,2-diazides, employing Cu $(acac)_2$ as an effective azide transfer reagent[28] (Scheme 1c). It is worth noting that all of the aforementioned reactions proceed through the formation of the β-azido carbon-centered radical, a common intermediate *in situ* generated by the addition of an electrophilic N_3 radical to an alkene, which is capable of participating in various subsequent radical transformations as a nucleophilic species.

Results and discussion

Inspired by these elegant works of Lin,[26,27,29] Xu,[28,30] and others,[31] we envisioned that the abovementioned nucleophilic β-azido C-centered radical intermediate could be chemo- and regioselectively cross-coupled with the electron-deficient heteroarene, allowing further oxidation and deprotonation for the rapid and diverse synthesis of alkylazidated heteroarenes (Scheme 1d). However, competitive side reactions are expected to occur during the synthesis, interfering with the desired transformation (Scheme 1e). They are as follows: (1) dimerization *via* radical homocoupling[32] owing to the instability of the β-azido alkyl radical intermediate; (2) manganese(II)-mediated alkene 1,2-diazidation reactions;[26] and (3) the formation of the β-azido Ritter intermediate from the incipient β-azido alkyl radical through sequential single-electron oxidation, followed by nucleophilic addition by MeCN.[33] Herein, we report an unprecedented azidoalkylation of heteroarenes enabled by Mn-electrocatalysis. This three-component reaction efficiently constructs structurally valuable azido-containing alkylated heteroarenes from simple starting materials in a single step, and the products obtained can be readily transformed into 1,3-amino alcohols, a class of compounds of considerable interest to synthetic chemists.[34]

We tested the viability of our proposed approach employing 9-benzyl-6*H*-purine (**1a**, 0.2 mmol) and allyltrimethylsilane (**3a**, 0.4 mmol) as the substrates, NaN_3 (0.4 mmol) as the azide source, and $MnBr_2{\cdot}4H_2O$ (5 mol%) as the mediator. The reaction was carried out using an undivided cell equipped with a graphite felt as the anode and a platinum plate as the cathode (Table 1, see also SI-2 for detailed optimization studies). After evaluating various reaction conditions, we were pleased to find that conducting the reaction at a constant current of 5 mA for 5 hours at room temperature under an N_2 atmosphere using a solvent mixture of CH_3CN/TFA (3.0 mL/0.2 mL) and *n*-Bu_4NOAc as the supporting electrolyte successfully resulted in an isolated yield of 92% for the desired product **4a** (entry 1). Changing the azide source from NaN_3 to $TMSN_3$ decreased the yield of **4a** to 85% (entry 2). The choice of solvent was critical for the reaction efficiency, and the mixed solvent system (CH_3CN/TFA, 15/1, 3.2 mL) gave the highest yield. When MeCN and AcOH were used as solvents, the reaction did not occur, while with MeOH, DMF and MeCN/HOAc as solvents diminished yields were obtained (entries 3 and 4). By varying the ratio of solvents in a solvent mixture MeCN/TFA, a decrease in the product yield was observed (entries 5 and 6). Direct electrolysis in the absence of the redox mediator $MnBr_2{\cdot}4H_2O$ led to a significant decrease in the yield of **4a** (49%), highlighting the significant role of $MnBr_2{\cdot}4H_2O$ (entry 7). Both direct and Mn-mediated azide oxidation are considered as possible pathways to initiate this reaction. Decreasing the loading of $MnBr_2{\cdot}4H_2O$ to 2.5 mol% reduced the yield to 70% (entry 8). When the reaction was tested using NaBr instead of $MnBr_2{\cdot}4H_2O$, a notable reduction in the yield of **4a** was observed. This outcome ruled out the involvement of a bromide-catalyzed azidoalkylation process (entry 9). With other manganese salts, such as $Mn(OAc)_2$, $MnCl_2$, and $Mn(OTf)_2$ as redox mediators, the desired product **4a** was obtained in yields of 81%, 70%, and 72%, respectively (entry 10). Upon changing the anode material to the Pt plate, the formation of **4a** significantly decreased, which can be attributed to the lower surface area of this electrode (entry 11). Comparable yields were obtained when the applied current was 2 mA for 10 hours or 10 mA for 3 hours (entries 12 and 13). When the reaction was carried out under an air atmosphere, the yield of **4a** decreased to 86% (entry 14). Attempts were made to run the system in the absence of an electrolyte, as NaN_3 (**2**) itself is a salt that allows the current to flow. Unfortunately, the yield of product **4a** dropped to 82% under electrolyte-free conditions (entry 15). As anticipated, the reaction was completely seized in the absence of electrical input (entry 16).

Table 1 Optimization of the reaction conditions[a]

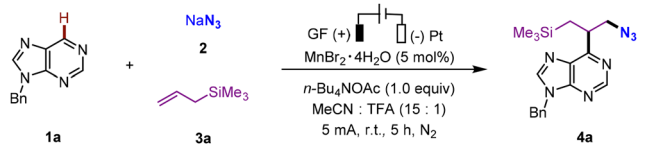

Entry	Variation from standard conditions	Yield[b] [%]
1	None	94(92)[c]
2	$TMSN_3$ instead of NaN_3	85
3	MeCN, HOAc, MeOH, or DMF as the solvent	nr, nr, 11, 38
4	MeCN/HOAc (15 : 1) as the solvent	5
5	MeCN/TFA (10 : 1) as the solvent	40
6	MeCN/TFA (20 : 1) as the solvent	65
7	Without $MnBr_2{\cdot}4H_2O$	49
8	2.5 mol% $MnBr_2{\cdot}4H_2O$	70
9	NaBr instead of $MnBr_2{\cdot}4H_2O$	56
10	$Mn(OAc)_2$, $MnCl_2$, and $Mn(OTf)_2$ instead of $MnBr_2{\cdot}4H_2O$	81, 70, 72
11	Pt(+)/Pt(−) instead of GF(+)/Pt(−)	40
12	2 mA for 10 h	90
13	10 mA for 3 h	92
14	Open flask	86
15	Without *n*-Bu_4NOAc	82
16	Without electric current	nr[d]

[a] Standard conditions: **1a** (0.20 mmol), NaN_3 (2.0 equiv., 0.40 mmol), **3a** (2.0 equiv., 0.40 mmol), $MnBr_2{\cdot}4H_2O$ (5 mol%, 0.01 mmol), *n*-Bu_4NOAc (1.0 equiv.), MeCN : TFA (15 : 1, 3.2 mL), GF anode, Pt cathode, 5 mA, undivided cell, at room temperature, under N_2 for 5 h (4.66 F mol^{-1}). [b] Determined by ^1H NMR analysis using CH_2Br_2 as the internal standard. [c] Isolated yield. [d] nr: no reaction. GF = graphite felt.

With the optimized conditions in hand, the substrate scope for purine was investigated (Table 2). To our delight, diverse 6*H*-purine nucleobases, 6*H*-purine nucleosides, and a 6*H*-purine nucleotide with different N9-substituents yielded the corresponding products (**4a–4ah**) in satisfactory yields (56–92%) with all reactions displaying high regioselectivity at the purinyl C6 position. A variety of functional groups, including alkyl (**4b–4i**), nitrile (**4k** and **4r**), ester (**4l**), phenyl (**4m**), alkene (**4n** and **4o**), alkyne (**4p**), ketone (**4q**), benzyl (**4r–4t**), halogen (**4t** and **4v**), alcohol (**4w**), and ether (**4y**), were well tolerated under the reaction conditions. Notably, many of these groups act as functional handles for subsequent synthetic modifications. Meanwhile, 9-benzyl-8-methyl-6*H*-purine and 9-benzyl-2-chloro-6*H*-purine participated in this reaction equally well, furnishing the related products **4u** and **4v** in 86% and 89% yields, respectively. It seemed that the electronic effect of the group on C2 or C8 had no obvious influence on the reaction efficiency. The acyclic purine nucleoside analogue bearing a 9-(2-hydroxyethyl), a 9-(2-acetoxyethyl), or a 9-acyclovir side chain was found suitable for this transformation, yielding the corresponding products **4w**, **4x**, and **4y** in 56%, 81%, and 86% yields, respectively. The single crystal X-ray diffraction analysis of **4t** was also performed to confirm the structure of the desired three-component coupling product. Subsequently, a variety of purine nucleosides were then probed (Table 2, **4z–4ag**). The 6*H*-purine nucleoside analogue, bearing a tetrahydropyranyl moiety at the N9 position, smoothly underwent the reaction, yielding the corresponding product **4z** in 71% yield. Moreover, ribosyl, 2′-deoxyribosyl, and arabinosyl purine nucleosides were compatible with the reaction conditions and yielded the desired products (**4ab–4af**) in 65–90% yields. To our delight, the labile purine ribonucleoside and 2′,3′-*o*-isopropylidene-protected purine ribonucleoside with unprotected hydroxyl groups also endured the present reaction conditions

Table 2 Purine scope exploration[a,b,c]

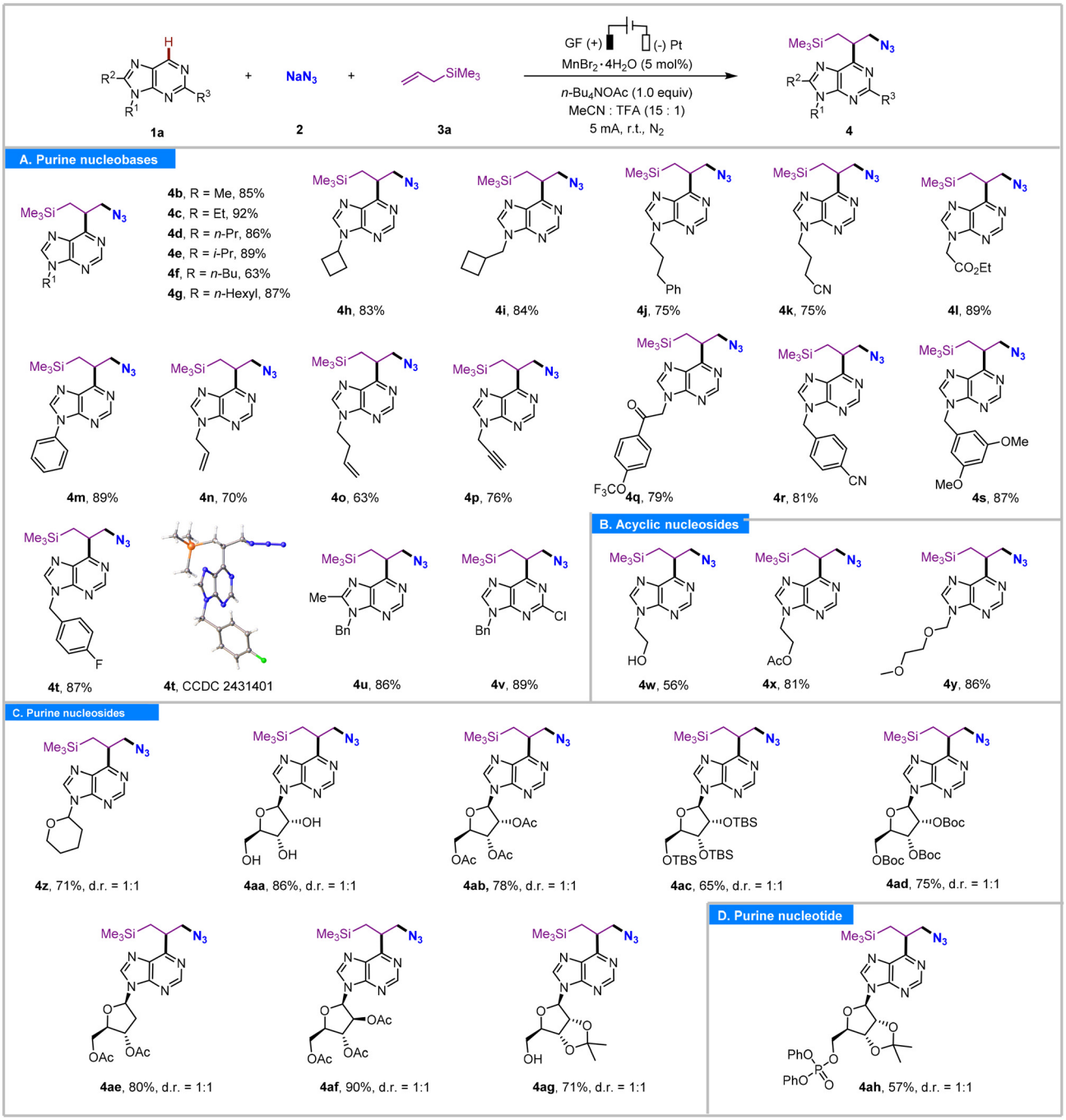

[a] Reaction conditions: **1a** (0.20 mmol), NaN_3 (2.0 equiv., 0.40 mmol), **3a** (2.0 equiv., 0.40 mmol), $MnBr_2{\cdot}4H_2O$ (5 mol%, 0.01 mmol), *n*-Bu_4NOAc (1.0 equiv.), MeCN : TFA (15 : 1, 3.2 mL), GF anode, Pt cathode, 5 mA, undivided cell, at room temperature, under N_2 for 4–6 h (3.73–5.59 F mol^{-1}). [b] Yields are based on the isolated products. [c] Diastereomeric ratio (d.r.) was determined by ^1H NMR spectroscopy.

(**4aa**, 86% yield; **4ag**, 71% yield). Meanwhile, this protocol was also effective with the purine nucleotide scaffold. Notably, the azidoalkylation of nucleotide selectively occurred at the C6 site of the purine subunit, yielding product **4ah** in 57% yield.

Encouraged by these results, the reaction generality with a wide variety of unactivated alkenes was also assessed (Table 3). Satisfactorily, allylic silanes such as allyldimethyl(phenyl) silane and allyltriphenylsilane successfully delivered the desired products **5a** and **5b** in 82% and 85% yields, respectively. Nonfunctionalized linear differently substituted aliphatic alkenes including monosubstituted, 1,1-disubstituted, trisubstituted, and tetrasubstituted alkenes underwent difunctionali-

Table 3 Alkene scope exploration[a,b,c]

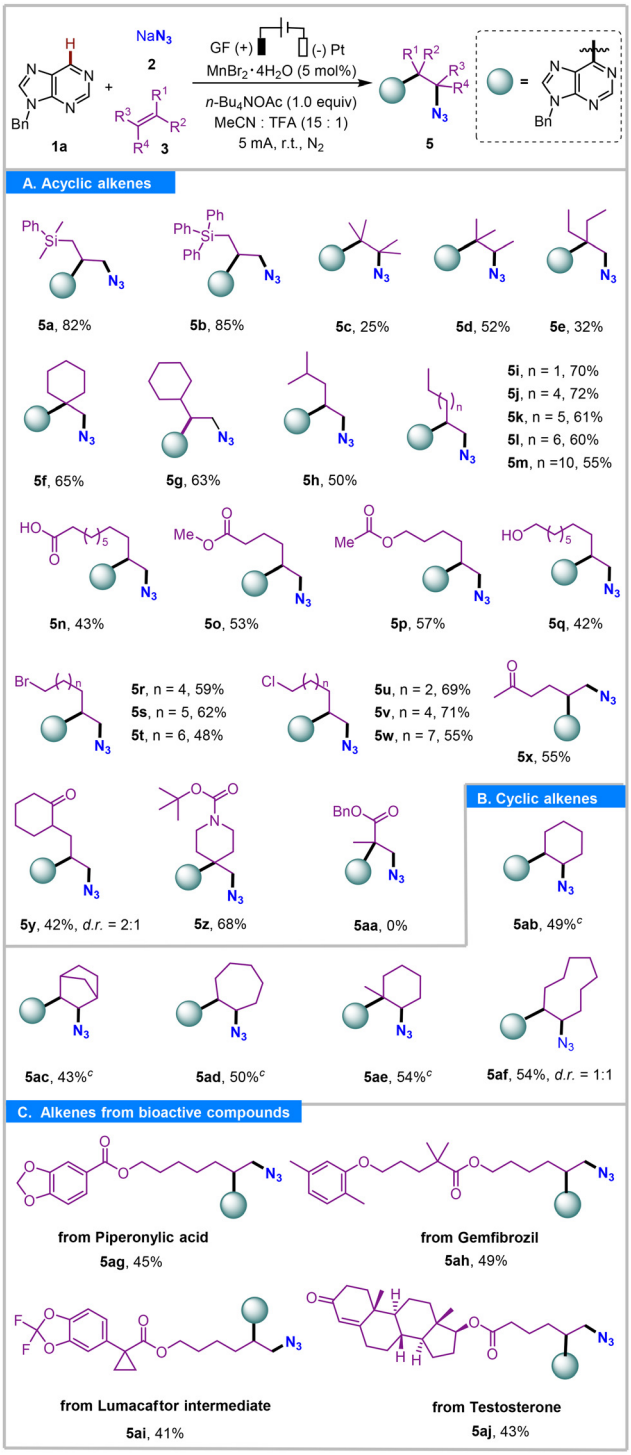

[a] Reaction conditions: **1a** (0.20 mmol), NaN_3 (2.0 equiv., 0.40 mmol), **3a** (2.0 equiv., 0.40 mmol), $MnBr_2{\cdot}4H_2O$ (5 mol%, 0.01 mmol), *n*-Bu_4NOAc (1.0 equiv.), MeCN : TFA (15 : 1, 3.2 mL), GF anode, Pt cathode, 5 mA, undivided cell, at room temperature, under N_2 for 5–8 h (4.66–7.46 F mol^{-1}). [b] Yields are based on the isolated products. [c] Products formed in >20 : 1 dr as determined by crude ^1H NMR.

zation smoothly yielding **5g–5m** (50–72%), **5e–5f** (32–65%), **5d** (52%), and **5c** (25%), respectively. The substituent carbon chain length exhibited an obvious influence on the reactivity of alkenes. As the carbon chain length increased, the product yields decreased (**5i–5m**, 55–72%). It is noteworthy that a large number of functionalized alkenes were also compatible with this system. Substituents susceptible to the S_N2 reaction with the azide anion, such as ester, alkyl bromide, alkyl chloride, and amide, were tolerated under the optimal conditions, yielding the corresponding products **5o** and **5p** (53% and 57%), **5r–5t** (48–62%), **5u–5w** (55–71%), and **5z** (68%). This could be due to the strong acidic reaction medium (TFA), which reduced the nucleophilicity of the N_3^-.[30] Substrates with oxidatively labile functional groups, such as carboxylic acid, alcohol, and enolizable ketone, were also compatible with the anodic electrolysis and resulted in products **5n** (43%), **5q** (42%), and **5y** (42%). In particular, the reaction with internal cyclic alkenes such as cyclohexene, norbornene, cycloheptene, 1-methylcyclohex-1-ene, and cyclononene gave the corresponding products (**5ab–5af**) in 43%–54% yields together with moderate to excellent diastereoselectivities (dr 1 : 1–>20 : 1). Unfortunately, the reaction with an electron-deficient alkene, such as an α,β-unsaturated ester, failed to yield the desired three-component product (**5aa**).

To our delight, the protocol was effective for a diverse range of complex alkenes derived from natural products and pharmaceutical molecules, including piperonylic acid, gemfibrozil, lumacaftor intermediate, and testosterone. The corresponding products (**5ag–5aj**) were obtained in moderate yields (45%, 49%, 41%, and 43%, respectively), which are attributed to the formation of unknown side products. Despite this, the approach remains noteworthy for its modularity and efficiency in constructing unique vicinal azidoheteroaryl scaffolds.

The synthetic versatility of this protocol was further demonstrated through the exploration of a broad range of heteroaromatics that are extremely valuable for drug discovery (Table 4). The quinolines bearing a substituent at the C4 position yielded the corresponding C2 azidoalkylated products (**7a** and **7b**) in moderate yields (59–61%). Meanwhile, 2-substituted quinolines reacted selectively at the C4 position, yielding products **7c** and **7d** in 54% and 45% yields, respectively. Isoquinolines with chloride, bromide, and phenyl substituents at the C4 or C6 position reacted well to provide C1 functionalized products **7e–7h** in 46–66% yields. Furthermore, pyrimidine and azauracil substrates were also found to be competent, producing three-component products **7i** and **7j** in 63% and 76% yields, respectively. Additionally, quinazolines underwent selective monoalkylation at C2 or C4 to furnish **7k** and **7l** in 33% and 55% yields, respectively. Other N-heteroarenes, such as quinoxaline, quinoxalinone, triazolo[4,3-*b*]pyridazine, benzo[*h*]quinoline, and phenanthridine also furnished **7m**, **7n**, **7o**, **7p**, and **7q** in 47%, 43%, 52%, 50%, and 57% yields, respectively. To highlight the applicability of the protocol, we investigated the late-stage direct C–H functionalization of several complex pharmaceutical derivatives. For instance, regioselective azidoalkylation of fasudil at the C2 position of the

Table 4 Heteroarene scope exploration[a,b]

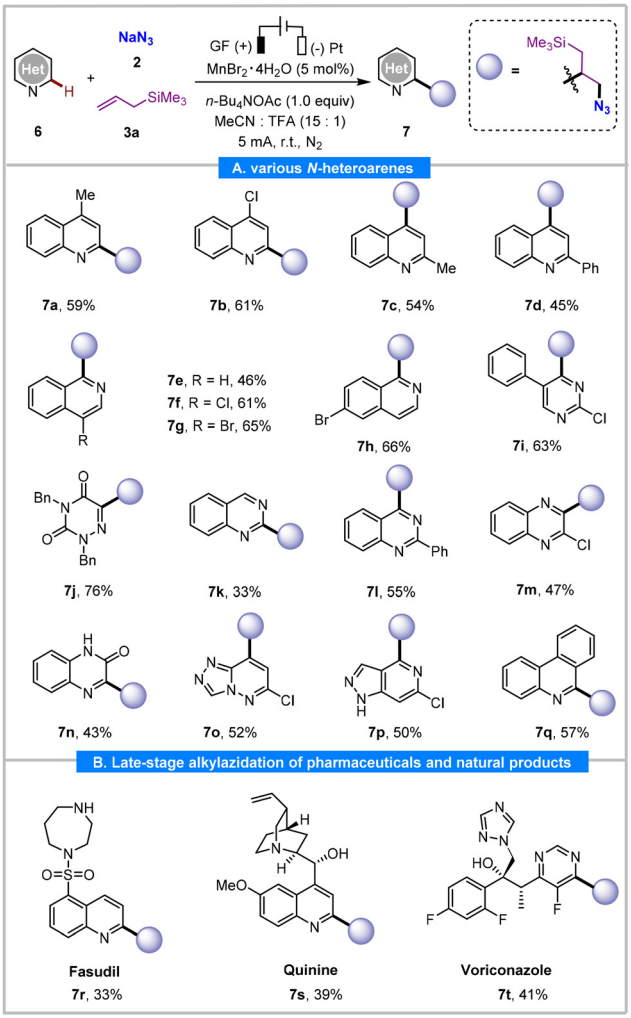

[a] Reaction conditions: **1a** (0.20 mmol), NaN_3 (2.0 equiv., 0.40 mmol), **3a** (2.0 equiv., 0.40 mmol), $MnBr_2{\cdot}4H_2O$ (5 mol%, 0.01 mmol), *n*-Bu_4NOAc (1.0 equiv.), MeCN : TFA (15 : 1, 3.2 mL), GF anode, Pt cathode, 5 mA, undivided cell, at room temperature, under N_2 for 5–10 h (4.66–9.33 F mol^{-1}). [b] Yields are based on the isolated products.

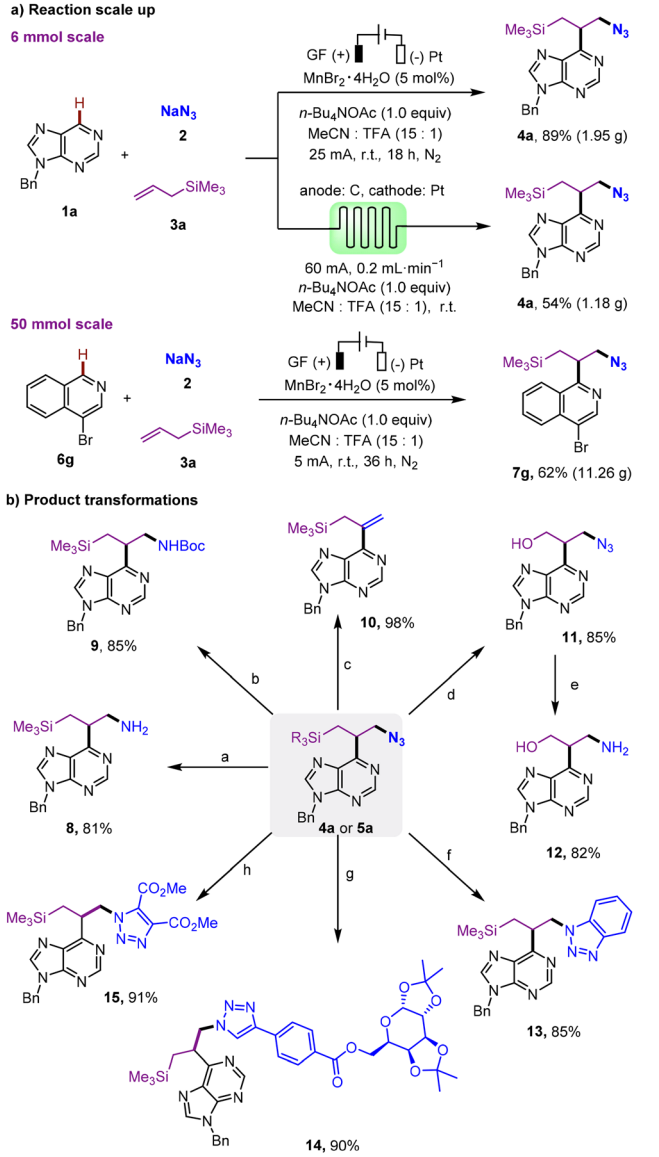

Scheme 2 Gram-scale synthesis and product transformations. Reaction conditions: (a) PPh_3 (1.5 equiv.), THF, 45 °C, 4.5 h then H_2O, 2 h; (b) Boc_2O (1.0 equiv.), Pd/C (0.05 equiv.), EA, r.t., 36 h; (c) *t*-BuOH (1.2 equiv.), THF, 80 °C, 1 h; (d) HBF_4 (2.0 equiv.), DCM, 0 °C, 2 h, then KF (2.0 equiv.), $KHCO_3$ (1.2 equiv.), H_2O_2 (0.7 mL) MeOH, THF, 8 h; (e) PPh_3 (1.5 equiv.), H_2O (5.0 equiv.), THF, 50 °C; (f) 2-(trimethylsilyl)phenyl trifluoromethanesulfonate (2.0 equiv.), CsF (2.0 equiv.), MeCN, rt, 4 h; (g) $CuSO_4{\cdot}5H_2O$ (0.2 equiv.), diacetone-D-galactose (1.5 equiv.), sodium ascorbate (0.4 equiv.), *t*-BuOH/H_2O/CH_2Cl_2, N_2, rt, 24 h; and (h) dimethyl acetylenedicarboxylate (2.0 equiv.) toluene, 110 °C, 2 h.

quinoline ring yielded **7r** in 33% yield. Quinine, bearing a reactive hydroxyl and a vinyl group, also tolerated the reaction conditions and underwent selective alkylazidation at the C2 position to give **7s** in 39% yield. The antifungal drug Voriconazole was also compatible with the reaction conditions, undergoing regio- and chemoselective azidoalkylation to afford **7t** in 41% yield. Notably, these complex pharmaceutical molecules exhibited a lower conversion rate, resulting in relatively lower yields of the target products (**7r–7t**).

To evaluate the practicality, this electrochemical radical cascade multicomponent Minisci reaction was tested on gram and decagram scales (Scheme 2). To our satisfaction, a gram-scale synthesis conducted in a batch reaction using **1a** (6.0 mmol, 1.26 g), NaN_3 (12.0 mmol, 0.78 g), and **3a** (1.90 mL, 12.0 mmol) yielded 1.95 g of **4a** with 89% yield (Scheme 2a). This was similar to the result from the small-scale reaction. The inherent green and sustainable features of the flow chemistry prompted us to explore the scale-up synthesis *via* a continuous-flow electrochemical microreactor (see SI Fig. S4 for details). Starting with 6 mmol of purine compound (**1a**), the desired product (**4a**) was obtained in 54% yield (1.18 g) after 24 hours in a microflow reactor, operating with a constant current of 60 mA and a flow rate of 0.2 mL min^{-1}. Notably, the

electrolysis of 4-bromoisoquinoline was successfully carried out on a decagram scale, yielding **7g** in 62% yield (11.26 g), demonstrating the scalability of the method.

The synthetic applications of the obtained azidoalkylation products were further investigated using **4a** as a model substrate to study the functional group derivatizations (Scheme 2b). The reduction of the azide group in **4a** using the Staudinger reaction with PPh_3 produced amine **8** (81% yield). The hydrogenation on Pd/C followed by *N*-protection with Boc_2O of **4a** conveniently produced **9** in 85% yield. A facile base-promoted dehydroazidation of **4a** provided C6-vinylpurine (**10**) in 98% yield. The dimethyl(phenyl)silyl group in compound **5a** was converted to a hydroxyl group in the presence of HBF_4, yielding alcohol **11** with an 85% yield. Notably, compound **11** can be converted into 1,3-amino alcohol **12** under mild reducing conditions with 82% yield. The copper(I)-promoted "click" reactions of **4a** with various alkynes, such as the Kobayashi benzyne precursor, dimethyl acetylenedicarboxylate, and natural terminal alkyne-containing compounds like diacetone-D-galactose, efficiently produced triazoles **13–15** in 85%, 90%, and 91% yields, respectively.

To obtain insights into the mechanism of this electrochemical multicomponent Minisci reaction, a series of control experiments were carried out (Scheme 3). Firstly, it was found that the addition of a radical inhibitor namely BHT markedly inhibited the product formation. The corresponding radical-trapping product **16** was isolated and characterized by NMR spectroscopy (see the SI), confirming the involvement of azido radicals in the reaction (Scheme 3a). Secondly, when the "radical clock" substrate, bisallylamine **17**, was used under standard conditions, the expected ring-cyclized product **18** was obtained exclusively in 47% yield. This result provided strong evidence supporting the presence of the azido radical and suggested that the reaction proceeded through a nucleophilic carbon-centered alkyl radical intermediate, which further underwent a Minisci-type nucleophilic radical addition to the C6 position of purine (Scheme 3b). Thirdly, electricity on/off experiments demonstrated that the reaction did not proceed in the absence of a constant current (Scheme 3c), ruling out a long radical chain mechanism. Fourth, side-by-side kinetic reaction studies using equimolar quantities of **1a** and **1a**-D yielded an intermolecular kinetic isotope effect (KIE) value of k_H/k_D = 1.1 (Scheme 3d), suggesting that the deprotonation process is fast and likely not the rate-determining step. Finally, we attempted the use of $Mn(OAc)_3{\cdot}4H_2O$ as the oxidant instead of electricity (Scheme 3e). The reaction with 2.0 equivalents of $Mn(OAc)_3{\cdot}4H_2O$ gave **4a** in 51% yield. Further addition of $Mn(OAc)_3{\cdot}4H_2O$ (2.0 equiv.) increased the yield of **4a** to 65%, which was still much lower than that obtained under electrolysis conditions. The advantages of Mn(II)-promoted electrochemical reactions include not only the use of a catalytic amount of $MnBr_2{\cdot}4H_2O$ but also enhanced sustainability, higher yields, improved efficiency, and reduced environmental impact.

Cyclic voltammetry studies were also performed. As shown in Fig. 1A, a solution of the azide anion in MeCN showed an irreversible onset oxidation potential at E_p = 0.54 V (*vs.* SCE) (curve b, Fig. 1A), which shifted to E_p = 0.76 V (*vs.* SCE) upon the addition of TFA (curve c, Fig. 1A). Mixtures of $Mn(OAc)_2$ with NaN_3 exhibited a notable reduction in the onset oxidation

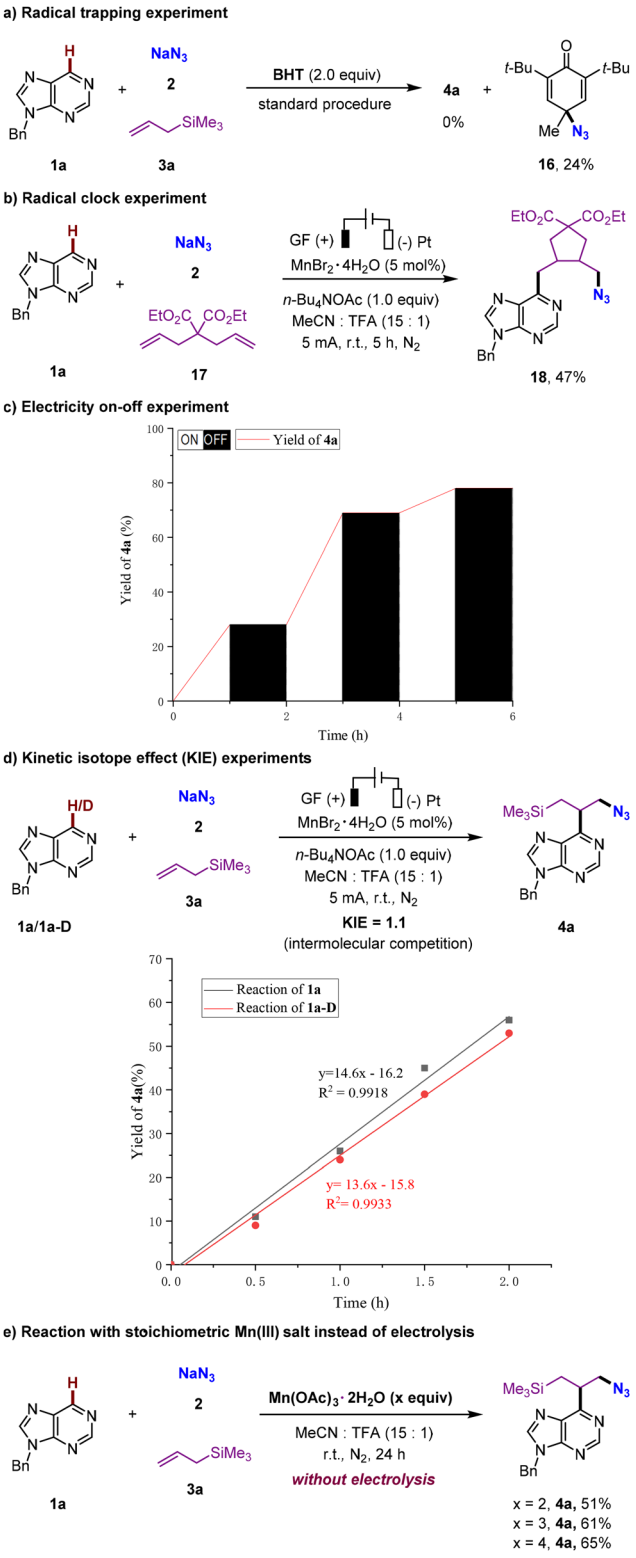

Scheme 3 Mechanistic studies.

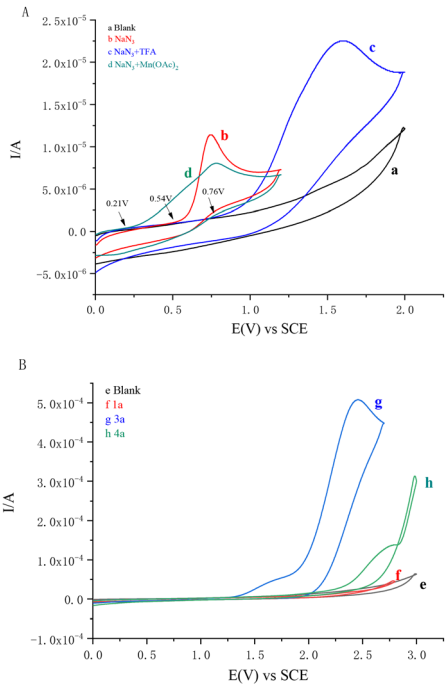

Fig. 1 Cyclic voltammograms obtained using a Pt disk as the working electrode, a Pt wire as the counter electrode, SCE as the internal reference electrode, 0.1 M $^{n}Bu_4NPF_6$, and a scanning rate of 100 mV s^{-1}: (A) curve a: blank; curve b: NaN_3 (5 mM); curve c: NaN_3 (5 mM) + TFA (1 mM); and curve d: NaN_3 (5 mM) + $Mn(OAc)_2$ (5 mM); (B) curve e: blank; curve f: **1a** (10 mM); curve g: **3a** (10 mM); and curve h: **4a** (10 mM).

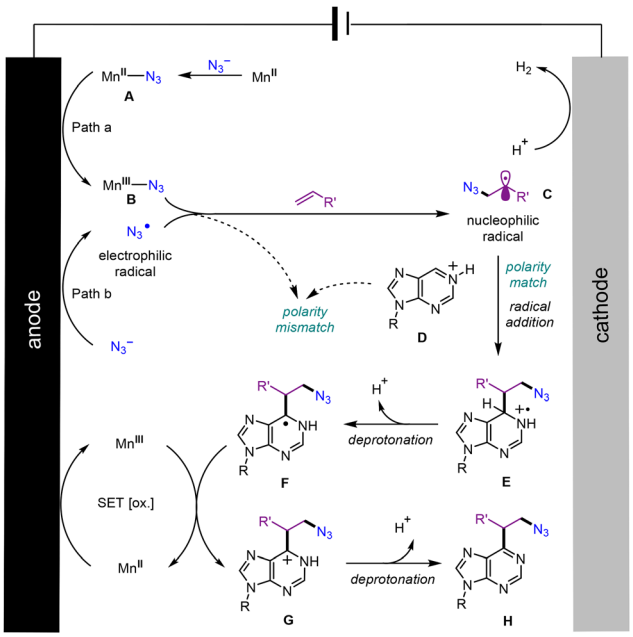

Scheme 4 Proposed mechanism of the reaction.

potential (E_p = 0.21 V *vs.* SCE) (curve d, Fig. 1A), which could be attributed to the formation of the Mn^{II}–N_3/Mn^{III}–N_3 couple.[26] Furthermore, the oxidation potentials of 9-benzyl-6*H*-purine **1a**, allyltrimethylsilane **3a**, and product **4a** are considerably higher than that of NaN_3 or Mn^{II}–N_3 (Fig. 1B). The data suggested that NaN_3 or Mn^{II}–N_3, rather than the alkene or purine substrates, is preferentially oxidized at the surface of the anode during the reaction. Clearly, the participation of the azido radical was supported by the results of the radical clock experiment (Scheme 3b).

A plausible mechanism was proposed according to our mechanistic studies and relevant literature reports (Scheme 4).[26,28] Initially, ligand exchange with sodium azide formed the Mn^{II}–N_3 complex **A**. Under electrochemical conditions, **A** underwent one-electron oxidation at the anode to generate the reactive Mn^{III}–N_3 intermediate **B**. The electrochemically generated **B** facilitated the formation of an azide radical through fragmentation. An alternative pathway involved the direct oxidation of the azide anion on the anode surface, resulting in the same outcome. Thereafter, the obtained electrophilic azido radical underwent chemoselective addition to an alkene, instead of the protonated heteroarene, to produce an alkyl radical intermediate **C**. Furthermore, Minisci-type C–H alkylation proceeded *via* radical addition of the alkyl radical **C** to a TFA-activated purine **D**, producing the radical cation intermediate **E**, which was converted to a neutral α-amino radical **F** by the loss of a proton. According to the KIE experiment, this step was not the rate-determining step. Subsequently, **F** was oxidized either by Mn^{III} or directly at the anode,[35] forming the cationic intermediate **G** through another single electron transfer (SET) process. Finally, the desired three-component coupling product **H** was obtained through the dehydrogenation of **G**. The acidic reaction system provided sufficient protons for hydrogen evolution at the cathode, which helped prevent the reduction of the manganese catalyst and maintain charge balance throughout the electrochemical process.

Conclusions

In summary, we have developed a general, green, and effective electrochemical oxidative three-component Minisci reaction of N-heteroarenes with unactivated alkenes and NaN_3 *via* a polarity-reversal pathway. This strategy provided a route to a diverse range of azidoalkylated heteroaromatics with significant medicinal relevance that remained largely unexplored. This reaction involved two highly regio- and chemoselective polarity-driven radical addition steps with the manganese catalyst acting as an electrochemical mediator by forming the Mn^{II}–N_3/Mn^{III}–N_3 couple. This electrocatalytic strategy features operational simplicity, mild reaction conditions, Earth-abundant Mn catalysis, wide substrate scope, and excellent functional-group compatibility. It facilitated direct and selective incorporation of important azide and heteroaryl groups across alkenes from simple starting materials. The application potential of the developed protocol was demonstrated through a suc-

cessful scale-up synthesis, late-stage functionalization of drug-based complexes, and downstream transformations. Mechanistic studies, including cyclic voltammetry, radical trapping, and radical clock experiments, provided a reasonable explanation for the proposed mechanism, which involved the electrochemical generation of the azidyl radical, followed by radical addition, nucleophilic addition, and deprotonative aromatization.

Conflicts of interest

There are no conflicts to declare.

Data availability

Supplementary information (SI): general information, experimental procedures, characterization data for all new compounds, and NMR spectra. See DOI: **https://doi.org/10.1039/d5qo01302j**.

CCDC 2431401 contains the supplementary crystallographic data for this paper.[36]

Acknowledgements

We gratefully acknowledge financial support from the Natural Science Foundation of Henan Province (232300421126), the National Natural Science Foundation of China (U22A20378), and the Natural Science Foundation of Xiamen Municipality (3502Z202571018). We also acknowledge the financial support from the Henan Key Laboratory of Organic Functional Molecules and Drug Innovation and the NMPA Key Laboratory for Research and Evaluation of Innovative Drug.

References

1 P. Bhutani, G. Joshi, N. Raja, N. Bachhav, P. K. Rajanna, H. Bhutani, A. T. Paul and R. Kumar, U.S. FDA approved drugs from 2015–June 2020: a perspective, *J. Med. Chem.*, 2021, **64**, 2339–2381.

2 X. Zhang, S. Li, F. Qiu, H. T. Ang, J. Wu and P. Jia, Photocatalyzed Minisci-type reactions for late-stage functionalization of pharmaceutically relevant compounds, *Green Chem.*, 2024, **26**, 3595–3626.

3 (*a*) R. S. J. Proctor and R. J. Phipps, Recent advances in Minisci-type reactions, *Angew. Chem., Int. Ed.*, 2019, **58**, 13666–13699; (*b*) W. Wang and S. Wang, Recent advances in Minisci-type reactions and applications in organic synthesis, *Curr. Org. Chem.*, 2021, **25**, 894–934; (*c*) G.-Y. Dou, Y.-Y. Jiang, K. Xu and C.-C. Zeng, Electrochemical Minisci-type trifluoromethylation of electron-deficient heterocycles mediated by bromide ions, *Org. Chem. Front.*, 2019, **6**, 2392–2397; (*d*) Q.-Q. Wang, K. Xu, Y.-Y. Jiang, Y.-G. Liu, B.-G. Sun and C.-C. Zeng, Electrocatalytic Minisci acylation reaction of *N*-heteroarenes mediated by NH_4I, *Org. Lett.*, 2017, **19**, 5517–5520.

4 (*a*) T. Li, K. Liang, Y. Zhang, D. Hu and C. Xia, Three-Component Minisci reaction with 1,3-dicarbonyl compounds induced by visible light, *Org. Lett.*, 2020, **22**, 2386–2390; (*b*) Y.-L. Su, G.-X. Liu, L. D. Angelis, R. He, A. Al-Sayyed, K. S. Schanze, W.-H. Hu, H. Qiu and M. P. Doyle, Radical cascade multicomponent Minisci reactions with diazo compounds, *ACS Catal.*, 2022, **12**, 1357–1363; (*c*) J. Q. Buquoi, J. M. Lear, X. Gu and D. A. Nagib, Heteroarene phosphinylalkylation via a catalytic, polarity-reversing radical cascade, *ACS Catal.*, 2019, **9**, 5330–5335; (*d*) Y. Lu, M. Li, Q. Feng, Z. Zhang, Z. Zhang, K. Lu, Z. Liu and X. Zhao, Visible-light-induced tandem reaction of quinoxalin-2(1*H*)-ones, alkenes, and sulfonyl chlorides, *Org. Biomol. Chem.*, 2024, **22**, 6799–6809; (*e*) Z. Wang, Photocatalytic difunctionalization of arylalkenes with quinoxalinones and dialkyl dithiophosphoric acids, *Org. Biomol. Chem.*, 2024, **22**, 8575–8579; (*f*) M. Zhang, J. Zhang, Y. Zhou, Y. He, J. Wu and D. Zheng, Photoredox-catalyzed three-component amidoheteroarylation of unactivated alkenes, *Org. Lett.*, 2023, **25**, 4113–4118; (*g*) C. Shi, L. Guo, H. Gao, M. Luo, X. Zhou, C. Yang and W. Xia, Three-component aminoheteroarylation of alkenes via photoinduced EDA complex activation, *Org. Lett.*, 2023, **25**, 7661–7666; (*h*) L. Lin, P. Wang, T. Dong, G. C. Tsui and S. Liao, Radical fluorosulfonyl heteroarylation of unactivated alkenes with quinoxalin-2(1*H*)-ones and related N-Heterocycles, *Org. Lett.*, 2023, **25**, 1088–1093.

5 M. Grammel and H. C. Hang, Chemical reporters for biological discovery, *Nat. Chem. Biol.*, 2013, **9**, 475–484.

6 G. C. Tron, T. Pirali, R. A. Billington, P. L. Canonico, G. Sorba and A. A. Genazzani, Click chemistry reactions in medicinal chemistry: applications of the 1,3-dipolar cycloaddition between azides and alkynes, *Med. Res. Rev.*, 2008, **28**, 278–308.

7 P. Thirumurugan, D. Matosiuk and K. Jozwiak, Click chemistry for drug development and diverse chemical–biology applications, *Chem. Rev.*, 2013, **113**, 4905–4979.

8 W. Xi, T. F. Scott, C. J. Kloxin and C. N. Bowman, Click chemistry in materials science, *Adv. Funct. Mater.*, 2014, **24**, 2572–2590.

9 H. C. Kolb, M. G. Finn and K. B. Sharpless, Click chemistry: diverse chemical function from a few good reactions, *Angew. Chem., Int. Ed.*, 2001, **40**, 2004–2021.

10 Z. Lao and P. H. Toy, Catalytic wittig and aza-wittig reactions, *Beilstein J. Org. Chem.*, 2016, **12**, 2577–2587.

11 C. Bednarek, I. Wehl, N. Jung, U. Schepers and S. Bräse, The staudinger ligation, *Chem. Rev.*, 2020, **120**, 4301–4354.

12 D.-J. Chen and Z.-C. Chen, Hypervalent iodine in synthesis. Part 54: One-step conversion of aryl aldehydes to aroyl azides using a combined reagent of (diacetoxyiodo)benzene with sodium azide, *Tetrahedron Lett.*, 2000, **41**, 7361–7363.

13 E. Nyfeler and P. Renaud, Intramolecular schmidt reaction: applications in natural product synthesis, *Chimia*, 2006, **60**, 276–284.

14 T. Uchida and T. Katsuki, Asymmetric nitrene transfer reactions: sulfimidation, aziridination and C–H amination using azide compounds as nitrene precursors, *Chem. Rec.*, 2014, **14**, 117–129.
15 (*a*) P. Sivaguru, Y. Ning and X. Bi, New strategies for the synthesis of aliphatic azides, *Chem. Rev.*, 2021, **121**, 4253–4307; (*b*) L. Ge, M.-F. Chiou, Y. Li and H. Bao, Radical azidation as a means of constructing C(sp^3)-N_3 bonds, *Green Synth. Catal.*, 2020, **1**, 86–120.
16 M. Shee and N. D. P. Singh, Chemical versatility of azide radical: journey from a transient species to synthetic accessibility in organic transformations, *Chem. Soc. Rev.*, 2022, **51**, 2255–2312.
17 S. Biswas, S. Ghosh and I. Das, A TEMPO–N_3 complex enables the electrochemical C–H azidation of *N*–heterocycles through the cleavage of alkoxyamines, *ChemSusChem*, 2025, **18**, e202402139.
18 Z. Liu and Z.-Q. Liu, An intermolecular azidoheteroarylation of simple alkenes via free-radical multicomponent cascade reactions, *Org. Lett.*, 2017, **19**, 5649–5652.
19 J. M. Lear, J. Q. Buquoi, X. Gu, K. Pan, D. N. Mustafa and D. A. Nagib, Multi-component heteroarene couplings via polarity-reversed radical cascades, *Chem. Commun.*, 2019, **55**, 8820–8823.
20 J. Chen, S. Zhu, J. Qin and L. Chu, Intermolecular, redox-neutral azidoarylation of alkenes via photoredox catalysis, *Chem. Commun.*, 2019, **55**, 2336–2339.
21 J. Shen, L. He, C. Liang, Y. Ouyang, X. Yue, H. Wu, J. Xu, X. Liu, Q. Zhu and P. Zhang, Photoinitiated multicomponent cascade reaction of *N*-heteroarenes with unactivated alkenes and trimethylsilyl azide, *Mol. Catal.*, 2022, **524**, 112330–112337.
22 Y. Sun, G. Song, Y. Yan, T. Kang, J. Dong, G. Li and D. Xue, Red-light-driven enantioselective Minisci-type addition to heteroarenes via recyclable semi heterogeneous catalysis, *Green Chem.*, 2025, **27**, 5315–5321.
23 E. B. Corcoran, J. P. McMullen, F. Levesque, M. K. Wismer and J. R. Naber, Photon equivalents as a parameter for scaling photoredox reactionsin flow: translation of photocatalytic C–N cross-coupling from lab scale to multikilogram scale, *Angew. Chem., Int. Ed.*, 2020, **59**, 11964–11968.
24 (*a*) Y. Zhang, Z.-L. Zhou, J.-H. Li and Y.-T. Li, Electrochemical difunctionalization of alkenes, *Chem. Rec.*, 2025, e202400263; (*b*) F. Xiang, D. Wang, K. Xu and C.-C. Zeng, Paired electrolysis enabled trifluoromethylheteroaromatization of alkenes and alkyne with trifluoromethyl thianthrenium triflate (TT-CF_3+OTf–) as a bifunctional reagent, *Org. Lett.*, 2024, **26**, 411–415; (*c*) W.-Q. Yan, M.-Y. Lin, R. D. Little and C.-C. Zeng, Electrochemical regioselective azidoiodination of alkenes, *Tetrahedron*, 2017, **73**, 764–770.
25 L. F. T. Novaes, J. Liu, Y. Shen, L. Lu, J. M. Meinhardt and S. Lin, Electrocatalysis as an enabling technology for organic synthesis, *Chem. Soc. Rev.*, 2021, **50**, 7941–8002.
26 N. Fu, G. S. Sauer, A. Saha, A. Loo and S. Lin, Metal-catalyzed electrochemical diazidation of alkenes, *Science*, 2017, **357**, 575–579.
27 J. C. Siu, G. S. Sauer, A. Saha, R. L. Macey, N. Fu, T. Chauvire, K. M. Lancaster and S. Lin, Electrochemical azidooxygenation of alkenes mediated by a TEMPO–N_3 charge-transfer complex, *J. Am. Chem. Soc.*, 2018, **140**, 12511–12520.
28 C.-Y. Cai, Y.-T. Zheng, J.-F. Li and H.-C. Xu, Cu-electrocatalytic diazidation of alkenes at ppm catalyst loading, *J. Am. Chem. Soc.*, 2022, **144**, 11980–11985.
29 J. C. Siu, J. B. Parry and S. Lin, Aminoxyl-catalyzed electrochemical diazidation of alkenes mediated by a metastable charge-transfer complex, *J. Am. Chem. Soc.*, 2019, **141**, 2825–2831.
30 Y.-T. Zheng and H.-C. Xu, Electrochemical azidocyanation of alkenes, *Angew. Chem., Int. Ed.*, 2024, **63**, e202313273.
31 (*a*) Y. Weng, X. Xu, H. Chen, Y. Zhang and X. Zhuo, Tandem electrochemical oxidative azidation/heterocyclization of tryptophan-containing peptides under buffer conditions, *Angew. Chem., Int. Ed.*, 2022, **61**, e202206308; (*b*) T. H. Meyer, R. C. Samanta, A. D. Vecchio and L. Ackermann, Mangana(III/IV) electro-catalyzed C(sp^3)-H azidation, *Chem. Sci.*, 2021, **12**, 2890–2897; (*c*) L. Niu, C. Jiang, Y. Liang, D. Liu, F. Bu, R. Shi, H. Chen, A. D. Chowdhury and A. Lei, Manganese-catalyzed oxidative azidation of C(sp^3)–H bonds under electrophotocatalytic conditions, *J. Am. Chem. Soc.*, 2020, **142**, 17693–17702; (*d*) J. Wu, Y. Dou, R. Guillot, C. Kouklovsky and G. Vincent, Electrochemical dearomative 2,3-difunctionalization of indoles, *J. Am. Chem. Soc.*, 2019, **141**, 2832–2837.
32 P. Doz and H. Schäfer, Transition between metallic and ionic bonding in the silicides of the alkali and alkaline earth metals, *Angew. Chem., Int. Ed. Engl.*, 1970, **9**, 158–159.
33 Y. Yu, Y. Yuan and K. Ye, Electrochemical synthesis of vicinal azidoacetamides, *Chem. Commun.*, 2023, **59**, 422–425.
34 (*a*) B. Raju, K. Mortell, S. Anandan, H. O'Dowd, H. Gao, M. Gomez, C. Hackbarth, C. Wu, W. Wang, Z. Yuan, R. White, J. Trias and D. V. Patel, N- and C-terminal modifications of negamycin, *Bioorg. Med. Chem. Lett.*, 2003, **13**, 2413–2418; (*b*) R. W. Bates and K. Sa-Ei, Syntheses of the sedum and related alkaloids, *Tetrahedron*, 2002, **58**, 5957–5978; (*c*) S. M. Lait, D. A. Rankic and B. A. Keay, 1,3-Aminoalcohols and their derivatives in asymmetric organic synthesis, *Chem. Rev.*, 2007, **107**, 767–796.
35 S. Wang, Q. Xue, Z. Guan, Y. Ye and A. Lei, Mn-catalyzed electrooxidative undirected C–H/P–H cross-coupling between aromatics and diphenyl phosphine oxides, *ACS Catal.*, 2021, **11**, 4295–4300.
36 CCDC 2431401: Experimental Crystal Structure Determination, 2025, DOI: **10.5517/ccdc.csd.cc2mm29n**.